originated within the camera shade. (They were in direct sunlight within 10 cm of the camera lens.) The remainder of the particles were of small angular dimension at relatively infinite distances from the camera. It is extremely likely that such particles are present on any Aerobee flight and probably cannot be eliminated completely even with extreme precautions. It may be that such particles could account for the stray light signals reported by Wallace and McElroy (*4*) which, however, did not seriously detract from their results. Similar particles have been observed in coronagraph experiments on Aerobee rockets at small angles from the sun (*5*). Discrete particles have been observed and photographed from manned spacecraft (*6*).

The most significant conclusion that may be drawn from the daytime rocket photographs is that the day sky brightness in the photographic spectral region over the altitudes covered is only slightly brighter than that of the night sky. Our data for day glow brightnesses are generally consistent with the values observed photoelectrically by Wallace and McElroy (*4*). Such observations of the stellar aspect (low brightness) can be made in the daytime as well as at night (*7*) but extreme precaution should be used in designing equipment for daytime low-brightness observations because sunlight is scattered from discrete particulate matter nearby and from rocket and spacecraft payloads.

D. C. EVANS
L. DUNKELMAN
Goddard Space Flight Center, National Aeronautics and Space Administration, Greenbelt, Maryland

References and Notes

1. *Kodak 2485 High-Speed Recording Film Data Release* (Eastman Kodak Company, Rochester, N.Y., 1967).
2. C. W. Allen, *Astrophysical Quantities* (Athlone Press, Univ. of London; Oxford Univ. Press, New York, ed. 2, 1963).
3. F. E. Roach, *Space Sci. Rev.* **3**, 512 (1964); personal communication.
4. L. Wallace and M. B. McElroy, *Planet. Space Sci.* **14**, 677 (1966).
5. R. Tousey, M. J. Koomen, R. E. McCullough, R. T. Seal, *NASA* (*Nat. Aeronaut. Space Admin.*) *SP-135* (1955).
6. J. A. O'Keefe, L. Dunkelman, S. D. Soules, W. F. Huch, P. D. Lowman, Jr., *NASA* (*Nat. Aeronaut. Space Admin.*) *SP-45* (1963), p. 342.
7. J. P. Hennes and L. Dunkelman, *J. Geophys. Res.* **71**, 755 (1966).
8. E. P. Ney and W. F. Huch, *Science* **153**, 297 (1966).
9. D. C. Evans and L. Dunkelman, *Astron. J.* **72**, 795 (abstract) (1967).
10. C. Wolff, *Science* **158**, 1045 (1967).
11. G. Newkirk, Jr., *Planet. Space Sci.* **15**, 1267 (1967).

9 April 1969

Convergence and Strain Waves Caused by a Submerged Turbulent Disturbance in Stratified Fluids

Abstract. *Short bursts of submerged turbulent mixing in stratified water (everywhere denser below than above) is shown to cause waves of surface convergence, divergence, and strain. Quantitative data are given for four experiments.*

The phenomenon of "wake-collapse," caused by the passage of a submerged self-propelled body in a stratified fluid was initially reported in 1963 (*1*). The submerged turbulently mixed wake first expands due to turbulent momentum. It then reaches a vertical maximum. This is followed by a vertical contraction (collapse) accompanied by continued spreading horizontally. The collapse phase is an efficient generator of internal waves in the stratified fluid (*1, 2*). The phase of wake collapse for the time between the initiation of submerged turbulent mixing and the time of maximum vertical expansion of the wake, before it starts to collapse, has been considered earlier (*1, 3, 4*).

The present experiments yield data on the approximate maximum convergence and strain that reach the surface and travel outward from a point above a submerged turbulent disturbance. The apparatus consisted of a transparent cell 2.5 cm thick, 7.3 cm deep, and 30 cm long with internal wave dampers at the ends. The cell was filled with water between top and bottom copper strips, and stratification was introduced by cooling the bottom and heating the top with thermoelectric devices. A brief and repeatable turbulent disturbance, centered and 4.5 cm below the surface, was used to simulate the passage of a self-propelled body perpendicular to a narrow "slice" of stratified fluid (*3, 4*). Thermistors at positions along and near the upper surface measured wavelike convergence and divergence flows as

Table 1. Vertical profiles of temperature and Väisälä-Brunt period, specifying four different water stratifications used for the experiments z, depth; Θ, temperature; T, period; i, imaginary.

	Experiment a		Experiment b		Experiment c		Experiment d	
z (cm)	Θ (°C)	T (sec/cy)	Θ (°C)	T (sec/cy)	Θ (°C)	T (sec/cy)	Θ (°C)	T (sec/cy)
0	50.0	2.9	29.5	6.3	22.2	15.0	17.2	i
1	40.0	3.7	25.8	6.7	21.1	15.0	17.6	i
2	32.5	4.4	22.9	7.5	20.1	15.0	17.7	i
3	27.3	5.4	20.5	8.9	19.3	15.0	17.4	19.0
4	22.4	6.3	17.8	9.7	18.5	15.0	16.7	14.0
4.5	19.5	6.8	16.6	9.8	18.1	15.0	15.9	13.1
5	18.5	7.4	15.5	9.9	17.7	15.0	15.2	12.3
6	14.3	8.2	12.5	10.0	16.7	15.0	13.2	11.7
7	6.5	8.8	9.3	10.2	15.7	15.0	10.6	11.7

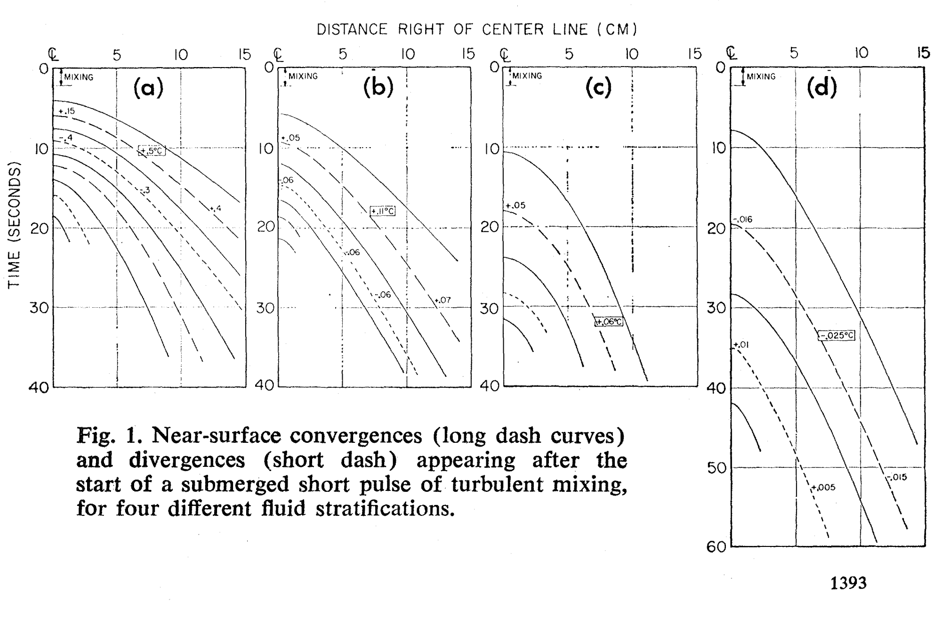

Fig. 1. Near-surface convergences (long dash curves) and divergences (short dash) appearing after the start of a submerged short pulse of turbulent mixing, for four different fluid stratifications.

they disturbed the near-surface equilibrium temperature gradient.

The results of four experiments are under the set of conditions given in Table 1. The water temperature Θ, and related Väisälä-Brunt period T, are given for various water depths. Phillips (*5*) indicates T is the natural period of oscillation of a parcel of fluid which has been given a small vertical displacement from its equilibrium position in a stratified fluid. To a good approximation

$$T = \frac{2\pi}{60\left(\frac{g}{\rho_0}\frac{\partial \rho}{\partial z}\right)^{1/2}} \text{ min/cycle}$$

where g is the acceleration of gravity, ρ_0 the reference density of the fluid, and $\partial\rho/\partial z$ the rate of change of density with depth. In experiments a and b, $\partial\rho/\partial z$ increased with depth and T was everywhere real. In experiment c, $\partial\rho/\partial z$ and T were both essentially constant. In experiment d, $\partial\rho/\partial z$ was slightly negative for $z < 2$ cm, and thus T was imaginary in this region. It was real for $z > 2$ cm.

Smoothed results of the four exploratory experiments are shown in Fig. 1, where the time after the start of a submerged pulse of turbulent mixing is plotted against distance from the vertical centerline ℄ of the cell. Convergence C near the surface is represented by the long-dash curves, divergence by the short-dash curves, and regions of zero convergence or divergence by the solid curves. (Curves to the left of ℄ are omitted because they would be mirror images of the ones shown.)

In experiments a to d the first convergence C_1, due to the simulated wake collapse, first reaches the surface at the ℄ where the pulse of submerged turbulent mixing started. The time for appearance of C_1 after the start of mixing was equal to $T(+13, -33$ percent) at the depth of initial disturbance $z = 4.5$ cm. This result is consistent with my earlier results (*3*).

In experiments a to c the maximum value of convergence C_m is located between 5 and 10 cm from ℄ on the C_1 curve. At these points C_m changes the equilibrium temperature $\Delta\Theta$ by $+0.50°$, $+0.11°$, and $+0.06°$C, respectively (Fig. 1). The maximum convergence $C_m = \Delta\Theta/(\partial\Theta/\partial z)$ was approximately 0.05, 0.04, and 0.05 cm for the three cases. The thermistors used for measuring $\Delta\Theta$ were below the surface a distance $\Delta z = 0.30$, 0.30, and 0.35 cm, respectively. Maximum vertical strain $S_v = C_m/\Delta z = 0.17$, 0.13, and 0.14 for experiments a, b, and c. Average S_v was about 0.15 which appears to be relatively insensitive to T when the geometry was not changed.

Near the surface S_v is obviously accompanied by a maximum horizontal surface strain S_h which may be of about the same order of magnitude as S_v. The locations of S_h for the experiments (Fig. 1) was between the long dashed curves and the solid curves, adjacent to the points of C_m. The slopes of the long dashed lines at the points of C_m and S_v gives a measure of the propagation velocity of these factors. The propagation of C_m, S_v (and S_h) = 0.86, 0.55, and 0.26 cm/sec for experiments a, b, and c, respectively.

Experiment d (Fig. 1) is unique in that T is imaginary for $z < 2$ cm and real for $z > 2$ cm. The center of the initial turbulent disturbance was at $z = 4.5$ cm where $T = 13.1$ sec/cycle. Thus, wake collapse was possible at mixer depth and produced convergence, divergence, and strain waves in the potentially unstable region near the surface. Maximum strain near the surface was found to be 0.16 which is essentially the same as for experiments a to c. For experiment d the propagation velocity of C_m, S_v, and S_h was about 0.31 cm/sec for the conditions of the experiment. It was judged impractical to check the results of d (as well as a to c) against theory, that is not fully developed, in an experimental note.

A. H. SCHOOLEY
Naval Research Laboratory, Washington, D.C. 20390

References

1. A. H. Schooley and R. Stewart, *J. Fluid Mech.* **15** (part 1), 83 (1963).
2. J. Wu, *Hydronautics Inc., Tech. Rep.*, No. 231-4 (1965); K. K. Wong, *ibid.*, No. 231-6, (1965); J. Wu, *ibid.*, No. 231-11 (1966).
3. A. H. Schooley, *Science* **157**, 421 (1967).
4. ———, *ibid.* **160**, 763 (1968).
5. O. M. Phillips, *The Dynamics of the Upper Ocean* (Cambridge Univ. Press, London, 1966), pp. 17, 163–170.

18 February 1969

Slumping Structures Caused by Organically Derived Gases in Sediments

Abstract. *The interstitial waters of many sediments are saturated with methane derived from the decay of included organic material. Further generation of methane or local pressure reduction results in sediment dilation and loss of sediment stability. The grains of sediment separated by gas behave in toto as an elastic fluid, and typical "slumping structures" result.*

Analysis and experiments have shown that clean sand, wet or dry, does not flow in response to stress. Rather, it falls along shear planes (*1*). The deformation of a mass of sand requires the expansion of that mass. The minimum expansion is required for the mass to fail along shear planes rather than by flowage. Flowage of a sand mass requires that any grain be free to move relative to the neighboring ones, a process requiring a large volumetric expansion that cannot be accomplished by stress alone. In order to fail under stress by flowage, sand grains must first be separated by some process other than stress.

Geologists have performed experiments in which sand was made to flow. These experiments, however, involved the use of interstitial plastic material, such as wax, so the flowage resulting under stress was actually the response of the wax to the stress field. The grains of sand were merely carried along within the wax. In the same way, sands containing adequate interstitial mud or clay can also fail by flowage if the sand grains are first separated so that individual grains do not become interlocked.

Despite the difficulty of accounting for the flowage of clean sands in response to stress, geologists have observed many examples of clean sands which have flowed, including spiral sand rolls, isolated sand rolls, sand crumpling, and sandstone dike injections. The fluid behavior of the sand masses is apparent in cases of sandstone dike injection, where fragile and sharp projections of shale on the containing walls of dikes often appear undisturbed, with their delicate points projecting into the invading sandstone mass. Many such fragments of shale are carried along as inclusions within the sand, their angular, fragile points